

Research report GAČR nr. 13-20031S 2015

Authors: D. Jašíková, M. Kotek, S. Fialová, F. Pochylý, M. Klíma, V. Kopecký

Keywords: Laser induced breakdown, Shadowgraphy, Cavitation bubble, Bubble wall interaction

Work schedule – 3rd year of the solution

Study of the influence of adhesion coefficient on the cavitation formation and the cavitation zone width

Introduction

Cavitation can be defined as a collection of effects connected to the origin, activities and collapse of macroscopic bubbles in liquid. In real applications cavitation bubbles are usually not separated. The bubbles create structures which acts collectively, however the essential elements of these structures are the individual bubbles.

The bubbles can be generated by several physically different mechanisms. The most obvious in nature is the hydrodynamics cavitation, where the bubbles are produced due to local pressure decrease caused by the flow acceleration in vicinity of obstacles. Acoustic cavitation is produced by imposing an intensive acoustic field into the bulk of liquid. The acoustic field causes the local tension of the liquid and its rupture. Energy deposition represents another possibility for the bubble generation. The high density energy source can be laser radiation or an electric arc. The high energy plasma causes the local evaporation of the liquid and bubble creation. The bubbles created by the energy deposition can be generated either by electric discharge or the optical breakdown.

The optical breakdown in liquid is usually produced by focusing of the laser light through suitably designed optics. The generation of cavitation bubble is the most delicate part of the each experimental setup as the bubble must be spherical and undisturbed. The setup that we used here comes out the laser with wavelength 532nm. The most spherical bubble shape exhibited with the assembly using concave mirror for the laser beam focusing. The laser beam was expanded before the focusing by Galilean beam expander. One difficulty connected with the generation of the laser



induced bubble is the limitation of its maximum size. The laser induced bubbles are usually produced in range of millimetres; however this requires high speed techniques for the bubble dynamics record.

In the first part of the solution we designed the LIB setup that enables single bubble generation of certain size. This setup had to be customized to the laser and consisted of the set of optical mirrors, lenses and optical table. The LIB run in the glass vessel filled with distilled water. In this part we also calibrated the bubble size to the laser output energy.

The second part of this aim contained to arrange the visualization setup. Here we used backlight visualization build on high speed camera. We chose three samples covered with ultra-hydrophobic surface for the comparison study. The glass was used as a reference sample.

There was observed and visualized cavitation bubble behaviour and dynamics as well as the impact on the ultra-hydrophobic surface.

Used samples

The investigated samples were prepared by the MUNI workplace, team of dr. Klima. There were selected three ultra-hydrophobic covered samples.

The first sample (Glass - A) was based on glass substrate. This was formed by first using plasma, precursor HMDSO, and thin layer of plasma precursor trimethyl boric acid (for reinforcement structure). This sample achieved static contact angle 160° on the dry surface. The wetted sample reached 150° and after cavitation process the value of static contact angle decreased to 145° . The static contact angle partly recovered after natural drying and stabilized on 155° . This sample creates very thin, no uniform air layer mostly coagulated into small bubbles.

The second sample (PE - C) – polyethylene substrate was continuously sprayed with UED[®] and cold Ar+O₂ plasma treated with initial static contact angle 158° , wetted surface 150° and after cavitation impact 145° and stabilized recovered to 150° .

The third sample (PE - A) – polyethylene substrate spray coated with nanopolymeric UltraEverDry[®] with initial contact angle 158° , after wetting 155° and after cavitation impact 151° .

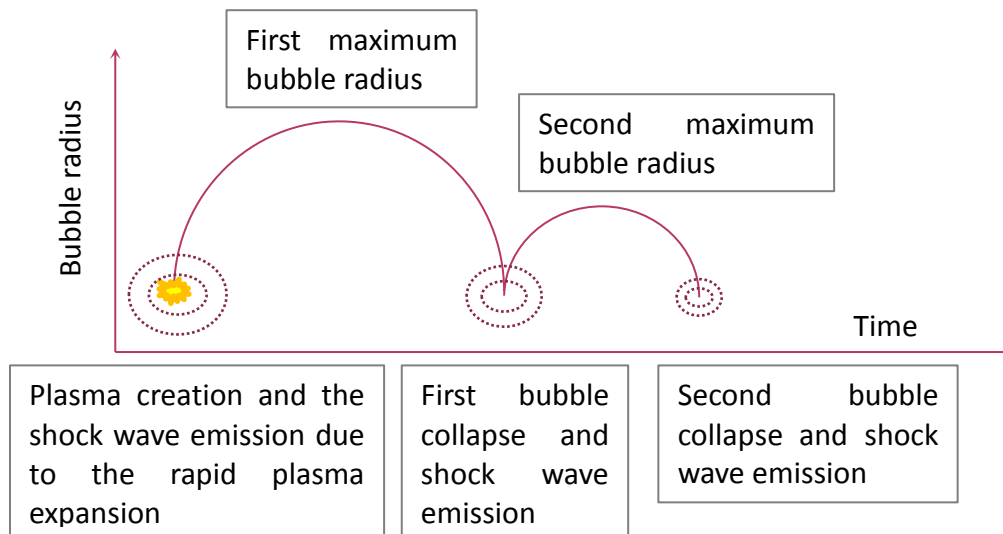
The polyethylene samples creates uniform air layer over the whole surface.

Here we used the untreated glass as the reference sample with static contact angle 60° .

Methods

Here we were focused on the behaviour of single cavitation bubble. For this purpose we selected the optic cavitation as suitable method that enables to generate bubble spatially precisely and with defined diameter. The liquid breakdown is caused by the local absorption of thermal and electromagnetic energy that leads to multi photon ionization followed with electron avalanche process, as visible plasma emission.





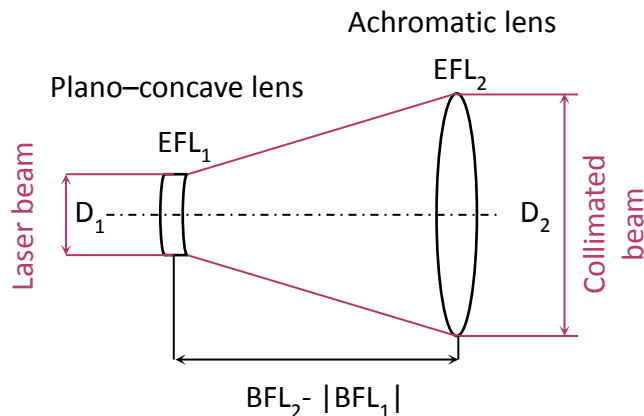
The mechanism of cavitation bubble behaviour in time.

The term of optical breakdown is generally used for short pulse exposures. In our experiments we used the laser of pulse width 10ns and the laser wavelength 532nm. The laser induced breakdown (LIB) leads to plasma expansion that is followed by audible acoustic wave, supersonic velocities, shock waves and cavitation effects. The laser pulse generates the dense plasma of temperatures (6000 – 15000)K and pressures (20-60)kbar. This initial effect evokes bremsstrahlung emission and electron-ion recombination that can be noticed as visible flash in broadband light spectrum. The plasma expansion is followed by the shock wave and during this sequence the liquid is vaporized and a cavitation bubble is growing. This bubble is filled with water vapour. The bubble collapse occurs during the second phase of the bubble lifespan. The collapse is caused by the reduction of interior pressure and cooling that is influenced by the external environment.

LIB setup

The 10ns width laser pulse was generated using Q-switched Nd:YAG NewGemini pulse laser. This laser worked with one cavity for single shot generation on the wavelength 532nm. The outlet diameter of the laser beam was 5mm with Gaussian characteristics of intensity. In our research setup we used EFL1 75mm, and EFL2 300mm, magnification of 4times. This setup is followed with the golden mirror of the focus 50mm. The focused laser beam created the laser point (radius<0.1mm). Due the losses in the optical path on each of optical elements, comparable to this, we had to increase the energy level that enters the whole system. The set output energy of the laser is taken in account in the relation to the bubble diameter.

The diameter of the laser beam was 5mm. the magnification of the Galilean beam expander was calculated according to $MP = \frac{EFL_2}{|EFL_1|}$.



The schema of the Galilean beam expander.

For the relation between input laser energy and the bubble size that was generated with our optical setup, we create the dataset of size – measurement.

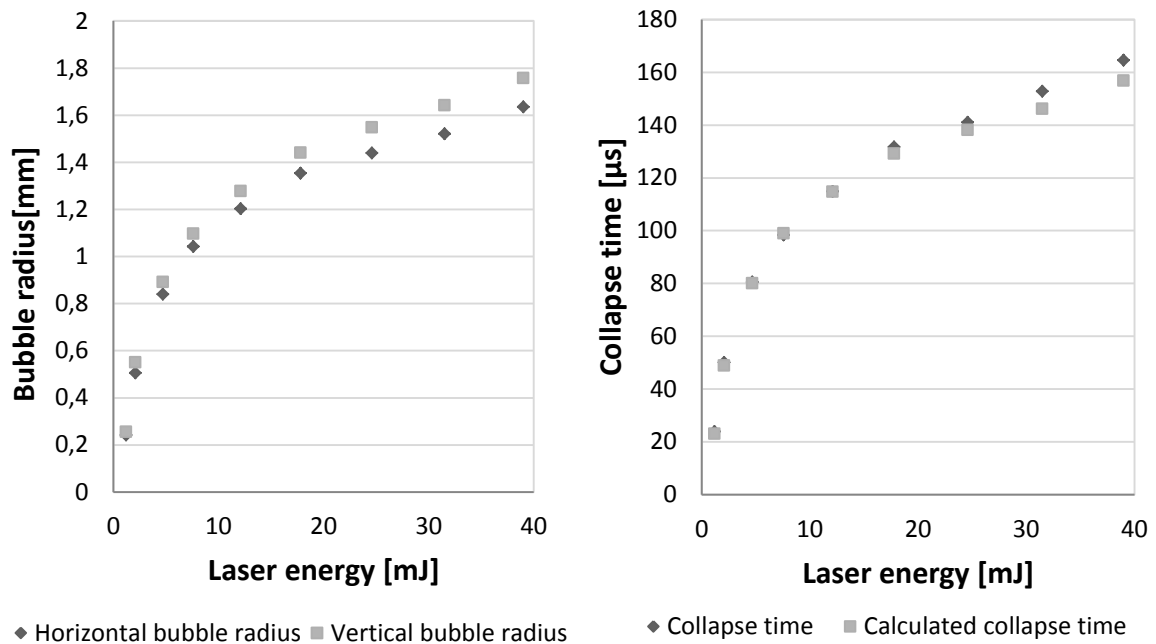
LIB calibration

The energy of the laser beam was set and measured with Ophir pyroelectric energy sensor. The dataset of at least 20 cavitation processes for statistic evaluation was captured. This maximum bubble size was detected in each image and it was related to the energy of the laser beam. The bubble size was measured in vertical and horizontal axis and the final value represents the average value. The increase of the laser energy causes the increase the horizontal value of the cavitation bubble size. This effect corresponds with the temporal and spatial plasma evolution at the very beginning of the process.

The process of LIB is not only characterized with the relation between the energy of the laser beam and cavitation bubble size, but also with the bubble dynamics. Rayleigh (1917) expressed the quotation that represent the collapse time of the bubble.

$$t_c = 0.915 \sqrt{\left(\frac{\rho_l \cdot R^2}{p_l - p_v} \right)}$$

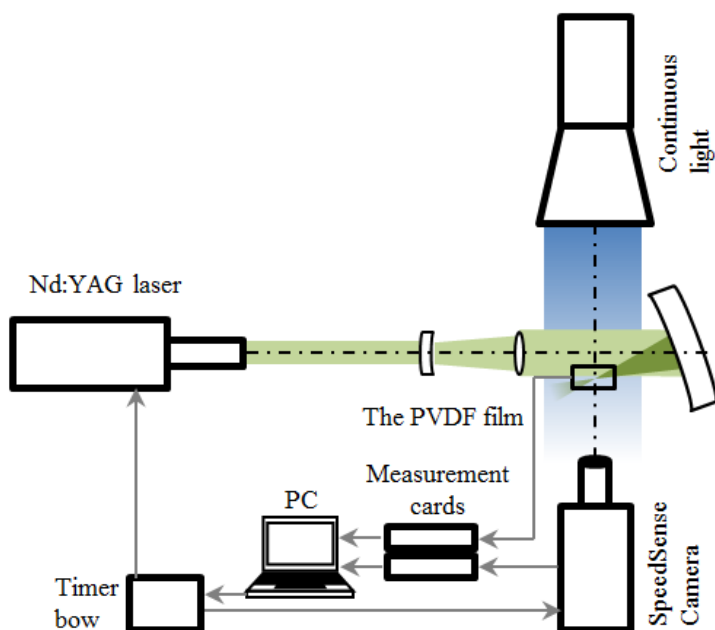
, where the ρ_l is the liquid density, R the radius of the bubble, p_l the atmospheric pressure in the surrounding liquid – 1×10^5 Pa and the p_v is the vapor partial pressure 2339 Pa for 20°C.



The graph of the relation between the cavitation bubble radius and the input laser energy and the graph of relation between the bubble collapse time and the input laser energy.

The relation between the energy of the laser beam and the cavitation bubble size is asymptotic. This means that further increase of laser energy does not lead to significant increase of the bubble size. With higher laser energy we recognized the negative influence of impurities and presence of segmentations on the bubble surface.

Visualization setup

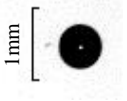
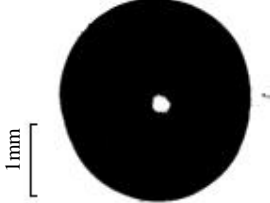
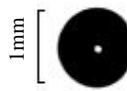
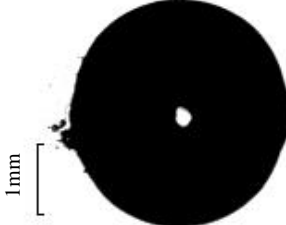
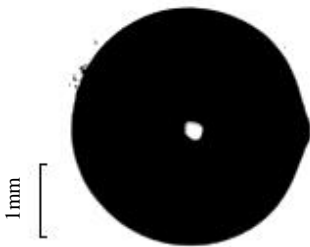
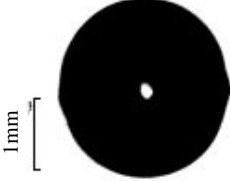


We used here the shadowgraph setup for the bubble visualization. This setup consists of the 1.5k Watt continuous daylight lamp of light temperature 5200K and 110k lux in the distance 1m far from the investigated object.

In the central horizontal axis, opposite to the light source was placed high speed CMOS camera SpeedSense from DantecDynamics. This camera is working on frequency 180kHz with resolution of (128x128)px or lower frequency with higher resolution up to (1280x800)px, and the dynamic range 12bit. The camera exposure



time was 1 μ s. The sub-pixel resolution was 20 μ m. The second important parameter for the visualization setup was the bubble lifespan. The camera setup is based on this information. It is important for the post trigger time setup.

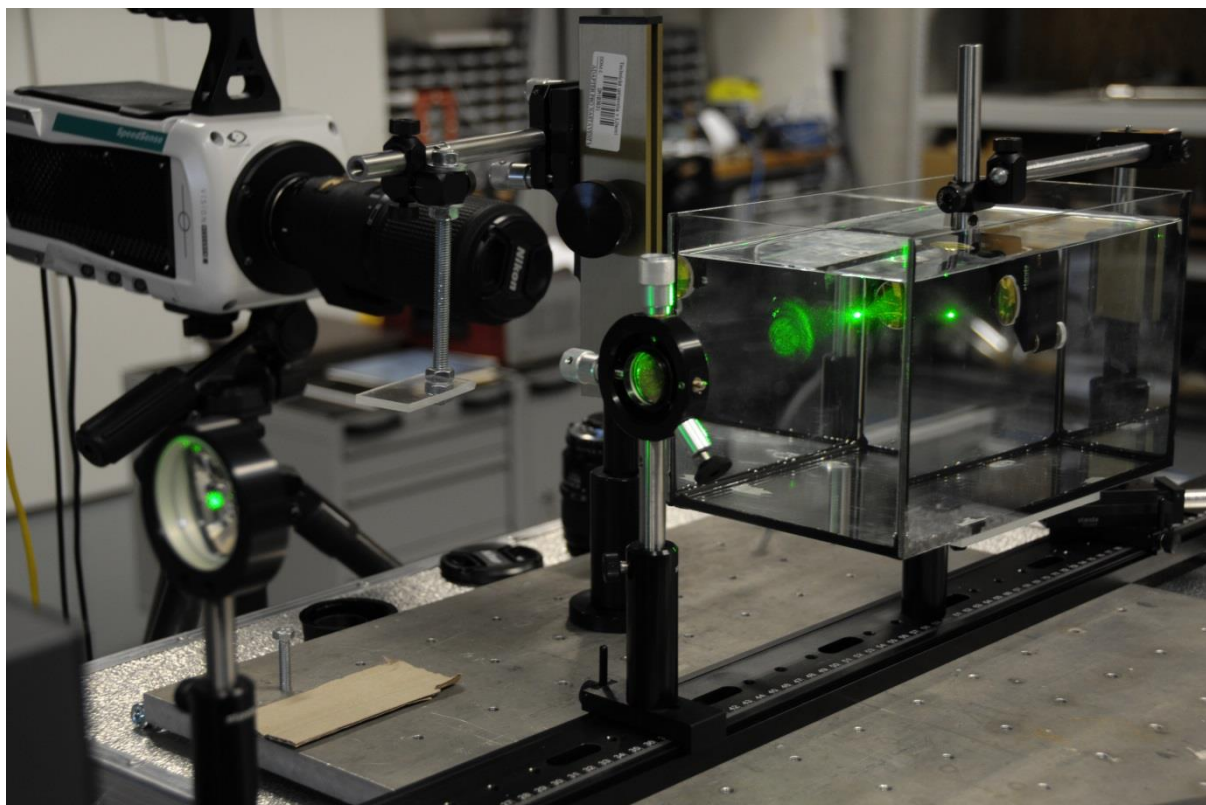
Input laser energy [mJ]	Cavitation bubble	Input laser energy [mJ]	Cavitation bubble
1,20		12,10	
2,09		17,80	
4,70		24,60	
7,60			

Calibration laser input energy with bubble size

As we successfully make the calibration pattern that gave us relation between the cavitation bubble size and the input laser energy, we could follow in our research that is mainly focused on the impact of the cavitation bubble on the surface. With our experimental setup we got the very precise equipment that enables the generation of the cavity bubbles time, geometrically and spatial defined.

In this project we selected the bubble size of 1mm that requires laser input energy of 2,09mJ.

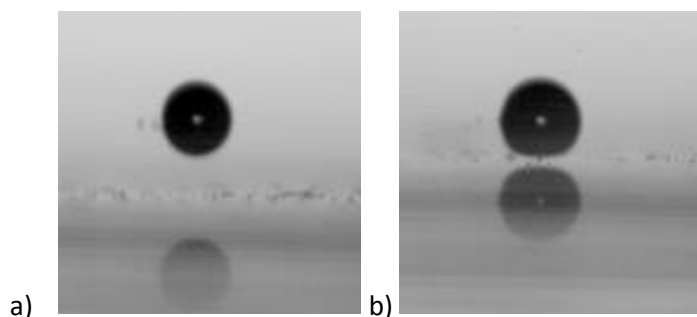




Laboratory view – the photo of the LIB setup and the laser beam expanded, collimated and focused into “spot” with concentrated energy to generate cavitation bubble.

Discussion / Interpretation of Results

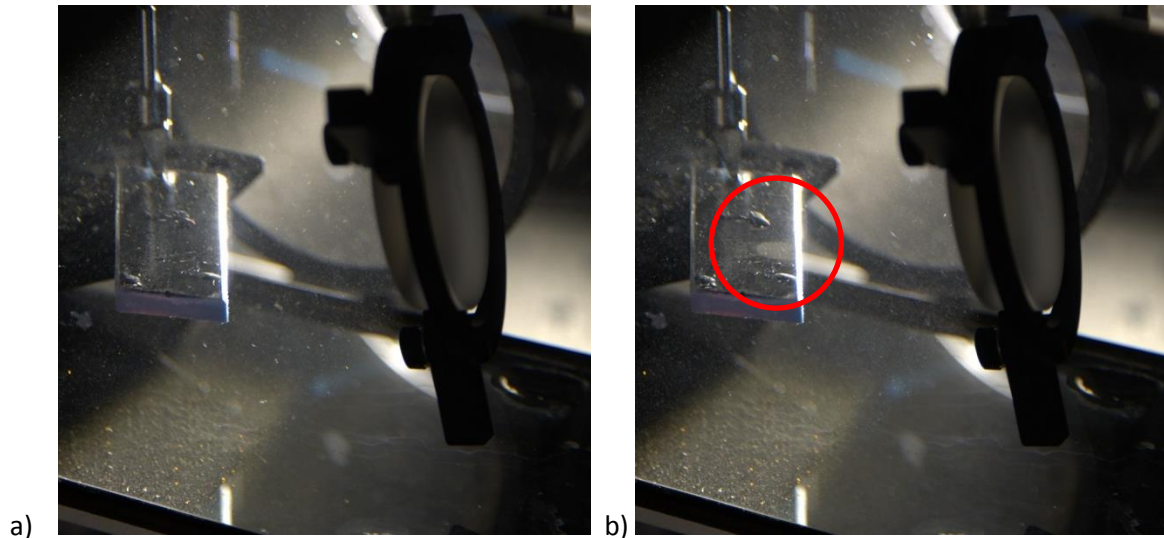
The LIB technique for single cavitation bubble enables very precise set of space and distance placement of the bubble. We have used two basic distances from the bubble centre to the surface. These distances come from the maximal bubble size. The first one can be described as one radius (1R) of the bubble and the second one is one diameter (1D) of the final bubble size.



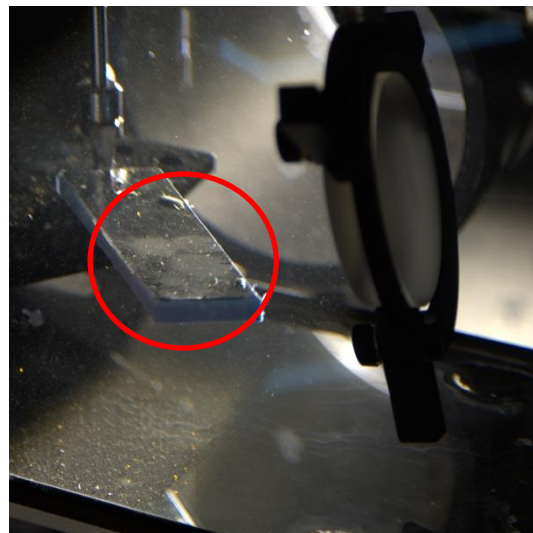
The camera record of fully developed cavitation bubble close to the glass wall in the distance a) 1R and b) 1D. There was placed glass reference sample with the mirror effect.

The effect several cavitation bubbles can be seen in the photo below. The red circle marks the point, where the cavitation bubbles were generated close to the surface. Even thou the cavitation bubble reached round 1mm of the maximum size, the impacted area on the ultra-hydrophobic surfaces reached almost 7mm.

We tested 10 cavitation bubbles in each distance and after the testing, there were significant reduces of the air film on the surface, anyway after sample draying the ultra-hydrophobic partly recovered.



The polyethylene sample placed into the cavitation chamber a) brand new sample with visible air layer, b) impacted region caused by cavitation bubbles.



Cavitation pattern created after three cavitation bubble points.

The camera records were analysed and for the interpretation for the results were selected several pictures that describe the effect.

	Time [μsec]	REF sample – glass	Sample Glass - A	Sample PE - A	Sample PE - C
0	0				
7	38.85				
11	61.05				
13	72.15				
15	83.25				
17	94.35				
21	116.55				

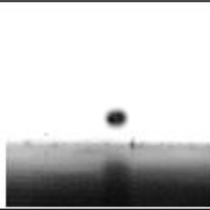
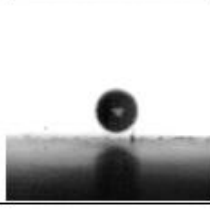
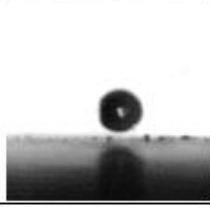
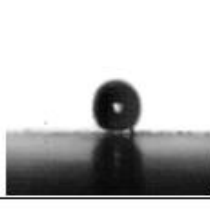
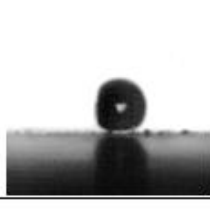
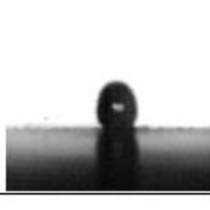
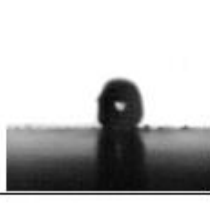
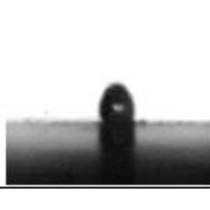
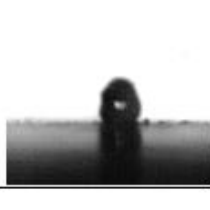
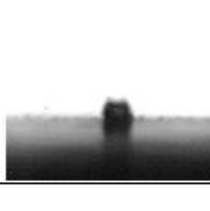
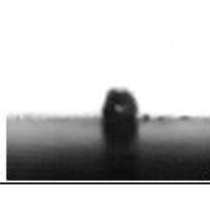
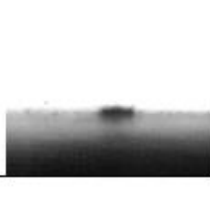
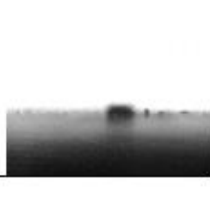
Shadowgraph visualization of the single cavitation bubble generated in the distance 1D from the surfaces.



	Time [usec]	REF sample – glass	Sample glass - A	Sample PE - A	Sample PE - C
0	0				
7	38.85				
11	61.05				
13	72.15				
15	83.25				
17	94.35				
21	116.55				

Shadowgraph visualization of the single cavitation bubble generated in the distance $1R$ from the surfaces.



	Time [usec]	1st bubble	5th bubble	10th bubble
0	0			
3	16.65			
9	49.95			
13	72.15			
15	83.25			
17	94.35			
19	105.45			

Shadowgraph visualization of the single cavitation bubble generated in the distance 1D from the surface of polyethylene sample C - continuously sprayed with UED® and cold Ar+O2 plasma treated.



The interaction of the cavitation bubble and the air film generated on the ultra-hydrophobic surface is noticeable on the geometry 1D – the bubble is in the distance one diameter bubble maximum size far from the surface. There can be seen significant effect of the air film attraction towards the cavitation bubble during the collapse phase of the cavitation process. The following impact force is absorbed with the air film. This effect increases the cavitation bubble impact radius up to 7D. The shockwave spreads over the air film and can be observed as oscillating pattern. The energy transmitted from the cavitation bubble to the air film is not absorbed immediately.

In the 1R regime is cavitation bubble generated close to the surface and it is part of air film, so the effect is not so significant, but the energy here is not attenuated and spread. Also the bubble shape is more triangular.

We also tested the repeatable generated cavitation bubbles and their effect on air film. The geometry was set as well as the distance between the bubble and surface. There was observed negative influence on the air film just on the first 5 cavitation bubbles. During the next cavitation process the air film was reduced. The effect of 10 cavitation bubbles is still reversible. There has been observed decrease of the static contact angle in the impacting area on the surfaces just after the cavitation process exposure. After the drying the surface recovered.

The progressive erosion caused by cavitation bubble also further influencing the ultra-hydrophobic surface. The damaged ultra-hydrophobic treatment works no more. This regime is irreversible.

We have also tested the ultra-hydrophobic surface that creates surface separated bubble in the contact with fluid (Sample Glass-A). The cavitation process was set above the surface bubble and it was observed the reducing of the surface bubble till it definitively disappeared.

The effect of cavitation process was proved with the static contact angle measurement that is mentioned in the initial part in the capture “Used samples”.

Conclusion

This part of the project was focused on the experimental study of the influence the cavitation formation on the ultra-hydrophobic surface. The solution was divided into three parts. In the first part set the LIB technique for the cavitation process generation. The LIB has many advantages and enables precise geometrical set up and also visualization.

There has been set the visualization setup in the second part. Here we used high speed shadowgraph. The image analysis and data interpretation also corresponds with this chapter.

The results proved that the cavitation process is affecting the ultra-hydrophobic surface via the air film.

References

1. Laser-induced breakdown in aqueous media, Kennedy, Paul K.; Hammer, Daniel X.; Rockwell, Benjamin A., Progress in Quantum Electronics, Volume 21, Issue 3, p. 155-248.



2. Vogel A, Busch S, Parlitz U. Shock wave emission and cavitation bubble generation by picosecond and nanosecond optical breakdown in water. *J. Acoust. Soc. Am.* 1996;100:148–165.
3. Vogel, A., et al., Energy balance of optical breakdown in water at nanosecond to femtosecond time scales, *Applied Physics B: Lasers and Optics* 68: 271-280 (1999).
4. M. Müller, W. Garen, S. Koch, F. Marsik, W. Neu and E. Saburov, Shock Waves and Cavitation Bubbles in Water and Isooctane generated by Nd:YAG Laser. *Experimental and Theoretical Results, Proc. SPIE Vol. 5399 (2004), 275-282.*
5. De-Bosset A, Obreschkow D, Kobel P, Dorsaz N, Farhat M. Direct effects of gravity on cavitation bubble collapse. In: *Proceedings of the 58 international astronautical congress. 2007. p. 1–5. 1AC-07-A2.4.04.*
6. D. Obreschkow, M. Tinguely, N. Dorsaz, P. Kobel, A. De Bosset, M. Farhat, (2013), "The quest for the most spherical bubble: experimental setup and data overview", *Experiments in Fluids*, 54, 1503
7. Müller, M.; Hujer, M.; Kotek, M.; Zima, P, Identification of collapse patterns of cavitation bubbles close to a solid wall, *Experimental Fluid Mechanics 2012. S. 494-497. - Liberec : Technical University of Liberec, 2012 / Vít T. ; Dančová P. ; Novotný P.*
8. Lauterborn, W., Optic cavitation, *Journal de physique*, **11**, 40, pp. 273-278, 1979.
9. P. K. Kennedy et al., Laser-induced breakdown in aqueous media, *Prog. Quant. Electr.* **21**, 3, pp. 155-248, 1997.
10. Jasikova, D., Muller, M., Kotek, M., Kopecky, V., The synchronized force impact measurement and visualization of single cavitation bubble generated with LIB, *International Journal of Mechanics* **9**, pp. 76-82, 2015.

